Ge substitutional defects and the $\sqrt{3} \times \sqrt{3} \leftrightarrow 3 \times 3$ transition in α-Sn/Ge(111)

2002 J. Phys.: Condens. Matter 14 7147

(http://iopscience.iop.org/0953-8984/14/30/305)

INSTITUTE OF PHYSICS PUBLISHING JOURNAL OF PHYSICS: CONDENSED MATTER

J. Phys.: Condens. Matter **14** (2002) 7147–7154 PII: S0953-8984(02)36291-X

Ge substitutional defects and the $\sqrt{3} \times \sqrt{3} \leftrightarrow 3 \times 3$ transition in α-Sn/Ge(111)

José Ortega[1], Rubén Pérez[1], Leszek Jurczyszyn[1,2] and Fernando Flores[1]

[1] Departamento de Física Teórica de la Materia Condensada, Universidad Autónoma de Madrid, E-28049 Madrid, Spain
[2] Institute of Experimental Physics, University of Wroclaw, Pl. Maksa Borna 9, 50–204 Wroclaw, Poland

Received 26 April 2002
Published 17 July 2002
Online at stacks.iop.org/JPhysCM/14/7147

Abstract

The structure and energetics of Ge substitutional defects on the α-Sn/Ge(111) surface are analysed using density functional theory molecular dynamics simulations. An isolated Ge defect induces a very local distortion of the 3×3 reconstruction, confined to a significant downwards displacement (-0.31 Å) at the defect site and a modest upward displacement (0.05 Å) of the three Sn nearest neighbours with partially occupied dangling bonds. Dynamical fluctuations between the two degenerate ground states yield the sixfold symmetry observed around a defect in the experiments at room temperature. Defect–defect interactions are controlled by the energetics of the deformation of the 3×3 structure: they are negligible for defects on the honeycomb lattice and quite large for a third defect on the hexagonal lattice, explaining the low-temperature defect ordering.

(Some figures in this article are in colour only in the electronic version)

The driving force behind the T-induced reversible $\sqrt{3} \times \sqrt{3} \leftrightarrow 3 \times 3$ phase transition observed for $\frac{1}{3}$ ML coverage of Sn or Pb on Ge(111) has been under intense debate since its discovery in Pb/Ge(111) [1]. Following the early suggestions of surface Fermi wavevector nesting or electron correlations, leading to the formation of a charge density wave [1, 2] at low T, recent theoretical work indicates that the softening of a 3×3 surface phonon [3], associated with the electronic energy gain due to the Sn dangling bond (DB) rehybridization, plays a major role on this transition. The dynamical fluctuations model [4] associated with this soft mode provides a consistent account of the main experimental facts, in particular the similarities of and differences between the isovalent Sn/Ge and Sn/Si(111) systems [3].

Density functional theory (DFT) calculations for the α-Sn/Ge(111) surface predict that the ground state is a 3×3 reconstruction in which a third of the Sn adatoms are placed $\sim$0.3 Å higher than the other Sn adatoms [3–6]. In other words, out of the three 3×3

sublattices that form the $\sqrt{3} \times \sqrt{3}$ lattice [10], 'up' Sn adatoms (Sn_u) occupy one of these sublattices (say a), forming a 3×3 *hexagonal* lattice, while sublattices b, c are occupied by 'down' Sn adatoms (Sn_d) (forming a *honeycomb* pattern). These calculations also show that this reconstruction is correlated with a change in the surface electronic structure [5]: the Sn_u DB is now fully occupied while the other two Sn_d DBs share the remaining electron per 3×3 unit cell. STM experiments are naturally explained in terms of these different DB occupancies. At LT, below T_c, filled-state STM images show the 3×3 phase: bright spots occupy the 3×3 sublattice associated with the Sn_u DBs, while the other two sublattices, associated with the Sn_d DBs, are occupied by darker spots [7]. At RT, however, dynamical fluctuations of the Sn adatom heights, fast with respect to the STM scan speed, induce a $\sqrt{3} \times \sqrt{3}$ periodicity in the STM images.

While these models assume an ideal $\frac{1}{3}$ ML Sn surface coverage, point defects, with an average concentration of $3 \pm 1\%$ [10], are always present. 90% of these defects are Ge substitutionals (called Ge defects in the rest of the paper), while vacancies account for the other 10%. STM, a real-space experimental technique, has been the method of choice to get non-averaged information on the structure and distribution of these defects on Sn/Ge(111) [8–10] across a wide temperature range, covering the transition temperature T_c. There are three main experimental results:

(i) At RT, Ge defects are imaged as dark spots in the $\sqrt{3} \times \sqrt{3}$ lattice surrounded by six features (brighter than Sn adatoms away from defects) that correspond to the six nearest-neighbour (nn) Sn atoms.
(ii) At LT, most of the Ge defects occupy positions corresponding to the two honeycomb Sn_d sublattices b, c, with equal probability, and are therefore surrounded by three bright and three darker Sn nn.
(iii) At RT, Ge defects are randomly distributed over the three sublattices a, b, c.

These results have been considered as supporting evidence for an interpretation of the $\sqrt{3} \times \sqrt{3} \leftrightarrow 3 \times 3$ phase transition in terms of the interaction of the Ge defects [8–10]. One of the main ingredients in this argument is the sixfold symmetry assumed for the perturbation induced by an isolated defect. This sixfold symmetry (honeycomb, with one atom dark and two atoms bright in the three possible sublattices), suggested by the RT STM images, is, however, in contradiction with the hexagonal pattern (two atoms dark and one atom bright, with threefold symmetry) observed in the filled-state images below T_c. In order to explain the LT experimental results, a defect–defect interaction, with a temperature-dependent decay length $l(T)$ (e.g. $l(300\ \mathrm{K}) \simeq 11$ Å, $l(100\ \mathrm{K}) \simeq 100$ Å) has to be introduced. This long-range interaction would be responsible for the ordering of defects at LT on two of the three possible sublattices. Finally, the superposition of the perturbations induced by defects in these two sublattices would give rise to the 3×3 phase.

In this paper, we show that *ab initio* DFT-LDA MD simulations of Ge substitutional defects on the Sn/Ge(111) surface support a completely different point of view: both the structure and the ordering of the Ge defects at LT are induced by the ground state 3×3 reconstruction. In particular, we have studied the atomic geometry, the electronic structure and the energetics of one and two Ge defects in a large 9×9 unit cell. In the case of two defects, we have considered three cases, corresponding to the defects on first-, second- and third-nn positions. Our analysis shows that Ge defects at LT always create a threefold distortion around them, the simulated STM filled-state image showing three bright and three darker spots on the nn Sn atoms. The distortion is very local, affecting only to the Sn atoms which are nearest neighbours of the defects. We have also performed first-principles MD simulations of a 3×3 unit cell with one Ge defect. Our MD simulations indicate that the sixfold pattern observed around Ge defects

Table 1. Atomic vertical displacements of the adatoms (in Å), measured with respect to the 3×3 reconstruction, for a Ge defect in a 3×3 unit cell. For the Ge defect the displacement is referred to the position of one of the 'down' Sn atoms of the 3×3 reconstruction. Calculations have been performed with both the efficient local-basis Fireball96 code (F96) and a plane-wave code (CASTEP).

	Sn 'up'	Sn 'down'	Ge defect
PW	+0.04	+0.08	−0.31
F96	+0.02	+0.10	−0.32

in the RT STM images should be understood in terms of the RT dynamical fluctuations of the six nn Sn adatoms. These dynamical effects contribute, together with structural and electronic effects, to the enhanced brightness of the Sn atoms around the defect.

In our approach we calculate different defects using a Sn/Ge(111)-9×9 unit cell with a slab of four Ge layers and a layer of H atoms saturating the DBs of the deeper Ge layer (432 atoms in the unit cell). Both the H layer and the last Ge layer are kept fixed during the calculations to mimic the bulk continuation. In our calculations we have used an efficient molecular dynamics (MD) technique, the Fireball96 code [12], that allows us to analyse the large 9×9 unit cell that we have considered. We have checked that this code yields accurate surface geometries by comparing it with a plane-wave code (CASTEP) [11] for the case of the Sn/Ge(111)-3×3 reconstruction [5] and for the case of one Ge defect on a 3×3 surface unit cell (see table 1). These results confirm the quality of the calculations provided by the Fireball96 code and justify the wide use we are going to make of it in the rest of the paper. STM images are calculated from the *ab initio* electronic structure of the surface using the Keldysh–Green function formalism and considering a W tip (for details on the method and the application to the Sn/Ge(111)-3×3 system, see [7]).

Figure 1(a) shows the relaxed geometry obtained in our calculations for the α-Sn/Ge(111) surface with one Ge defect per 9×9 unit cell (3.7% concentration). The surface presents the 3×3 reconstruction with the Ge adatom on one of the two 3×3 sublattices (say b) that form the honeycomb pattern associated with Sn_d adatoms. Our simulations yield for the Ge substitutional a downwards displacement of 0.30 Å with respect to the original Sn_d position. The perturbation induced by the Ge defect is well localized, affecting only the three nn Sn_d adatoms (c-sublattice). These adatoms are displaced upwards $\sim$0.05 Å due to the transfer of charge from the Ge defect: the Ge DB is empty and each nn Sn_d DB gains $\sim 1/6$ electrons. The occupancy of the nn Sn_u DBs (a-sublattice) does not change (they are already fully occupied), and therefore their position is practically the same as in the 3×3 reconstruction free of defects. Figure 1(b) shows the calculated filled-state STM image for this geometry. Probably the most remarkable feature is the threefold symmetry of the image around the defect (only three of the surrounding Sn atoms are imaged as protrusions), in contrast with the sixfold symmetry assumed for the perturbation induced by the defect from the experimental RT STM images.

Notice that the solution shown in figure 1 is twofold degenerate: an equivalent solution is obtained by applying a symmetry operation that exchanges the two sublattices (a, c) occupied by the up and down Sn. This degeneracy will be important when discussing the effect of temperature on the surface geometry and its corresponding STM image.

Figures 2(a)–(c) display the relaxed adatom positions that we have obtained for the α-Sn/Ge(111)-9×9 surface with two defects on first-, second- and third-nn positions. In all the cases the 3×3 reconstruction adapts its particular geometry (out of a threefold-degenerate case) to the defect positions, in such a way that the two defects are placed on the two Sn_d sublattices forming a honeycomb pattern. When the Ge defects are second nn (figure 2(b)), they are on the

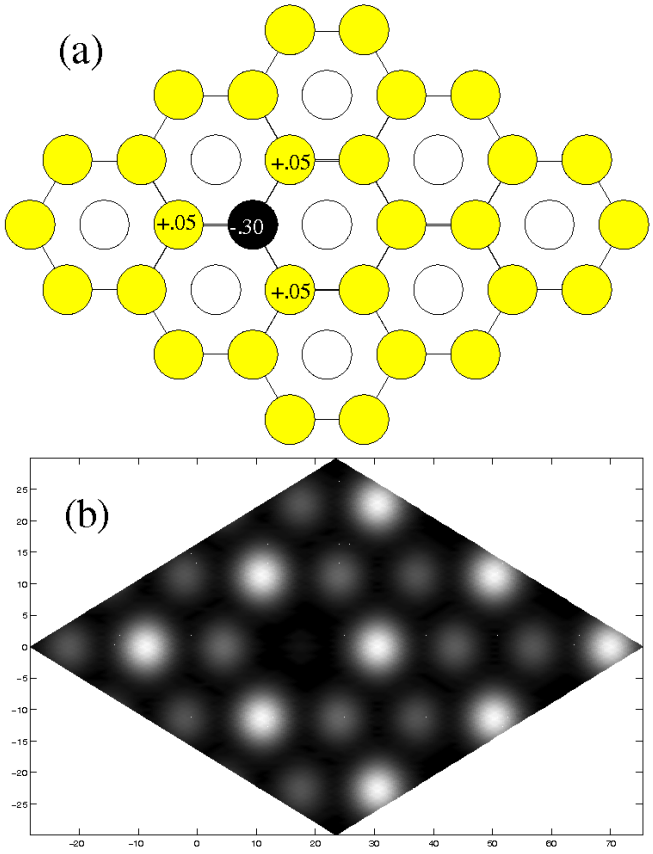

Figure 1. (a) Relaxed structure for the isolated defect. Only the vertical displacements (in Å) with respect to the ideal 3 × 3 structure which are larger than 0.01 Å are indicated. Notice that the distortion is confined to the defect site (black circle) and the three neighbouring Sn atoms with partially occupied DBs (grey circles). Sn atoms with fully occupied DBs are indicated by white circles. (b) A filled-state STM image for the isolated defect. The bright protrusions correspond to the fully occupied Sn DBs, and the grey ones to the Sn atoms with partially occupied DBs. The image reflects the threefold symmetry of the ground state structure of the defect.

same sublattice (say *b*), and the ground state is twofold degenerate: an exchange of the *a*- and *c*-sublattices gives a completely equivalent solution. In figures 2(a) and (c) the Ge defects occupy different sublattices and the solution is non-degenerate. As in the case of an isolated defect, the perturbation induced by the defects is localized essentially on the Sn adatoms that are nn to the defects. The total energies for the three cases shown in figure 2 are, within the accuracy of these calculations (∼20 meV/9 × 9 unit cell), the same, confirming the localized nature of the distortion induced by the Ge defects. It is remarkable that the sum of the upward displacements of all the neighbouring Sn adatoms is, in the three cases, very similar to the sum of the displacements induced by two independent defects (∼0.30 Å; see figure 1(a)). This result suggests a roughly linear relationship between the upwards displacement of a Sn adatom and the transfer of charge to its DB.

Coming back to the experimental STM data for the Ge defects on the Sn/Ge(111) surface, we first notice that our solution for a single defect (figure 1(b)) has a threefold and not a sixfold

symmetry, with the Sn atoms around the defect presenting two different types of displacements perpendicular to the surface. This apparent contradiction with the experimental data at RT can be resolved, however, considering the dynamics of the atoms around the defect. To this end, we have considered a 3×3 unit cell with a single substitutional and performed MD simulations at two different temperatures, $T = 180$ and 270 K. The initial conditions correspond to the positions of the relaxed structure of the defect (see table 1) and random velocities following a Maxwell–Boltzmann distribution. Then we follow the time evolution of the system integrating the equations of motion with the forces obtained from the DFT-LDA calculations. Figure 3 shows the time evolution of the z-coordinate of the three upper atoms (two Sn atoms and the Ge substitutional). These results show that Ge remains around its equilibrium site, while the two Sn atoms tend to exchange heights, in a very similar way to what we found for the $\sqrt{3} \times \sqrt{3}$ structure [4]. Therefore, the RT STM images of the six Sn adatoms that are nn to a Ge defect must represent a 50% average of Sn_u and Sn_d (displaced upwards by $\sim$0.05 Å w.r.t. normal Sn_d adatoms, and containing a sixth more electrons), while the RT STM images of Sn adatoms away from defects represent a $\frac{1}{3}Sn_u + \frac{2}{3}Sn_d$ average. This dynamical (plus charge transfer) effect explains in a simple way the different pattern observed at RT and LT on the STM images around a Ge defect (sixfold versus threefold symmetry) and also explains why Sn adatoms nn to a Ge defect appear in the RT STM images brighter than Sn adatoms in regions free of defects.

One should notice, however, that Ge substitutional defects tend to stabilize the 3×3 reconstruction locally and that the $\sqrt{3} \times \sqrt{3}$ structure associated with the dynamical fluctuations should appear at higher temperatures around these defects. This is clearly seen in the experimental STM image recorded by Melechko *et al* at 120 K [8]; here, the system shows a local 3×3 reconstruction around defects, while away from the defects STM images display the $\sqrt{3} \times \sqrt{3}$ symmetry.

We finally address the following question: why do Ge defects at LT occupy preferentially two 3×3 sublattices, with equal probability, and not the three of them or only one? Our results show that, on the α-Sn/Ge(111) surface, Ge substitutional defects transfer their DB charge to neighbouring Sn adatoms DBs and do not participate in the up/down dynamical fluctuations of the Sn adatoms at RT. Our results also show that at LT, when these fluctuations are suppressed, the stable configuration of the surface is a 3×3 reconstruction in which Ge defects occupy Sn_d positions; the defect–defect interaction is negligible (as long as they stay on Sn_d sublattices) and Ge defects occupy with equal probability any of the two Sn_d sublattices.

A third Ge defect initially located in the other sublattice (hexagonal) should be forced, when the temperature is lowered, either to present an upward displacement (contrary to what it does when it is isolated) or to deform its environment dramatically in order to move downwards. Any of these solutions would imply a significant energy cost (160 meV for the defect in a metastable upper position according to our calculations), that the system prefers not to pay, locking in all the substitutionals in a honeycomb lattice. We conclude that the ordering of Ge defects at LT is induced by the ground state 3×3 reconstruction and not the other way around: Ge substitutional defects are not the driving force of the $\sqrt{3} \times \sqrt{3} \leftrightarrow 3 \times 3$ transition in the α-Sn/Ge(111) surface.

In conclusion, our DFT-LDA total-energy and MD calculations show that the ground state geometry around a Ge substitutional defect corresponds to a very local distortion of the 3×3 reconstruction of the defect-free surface, confined to the defect site and the Sn nearest neighbours. The lattice deformation can be characterized by a downwards displacement of the Ge defect and upward displacement of the neighbouring Sn atoms with partially occupied DBs, with respect to the ideal 3×3 structure. This structural effect is correlated with the charge transfer from the defect DB to the DBs of these Sn atoms. This ground state configuration

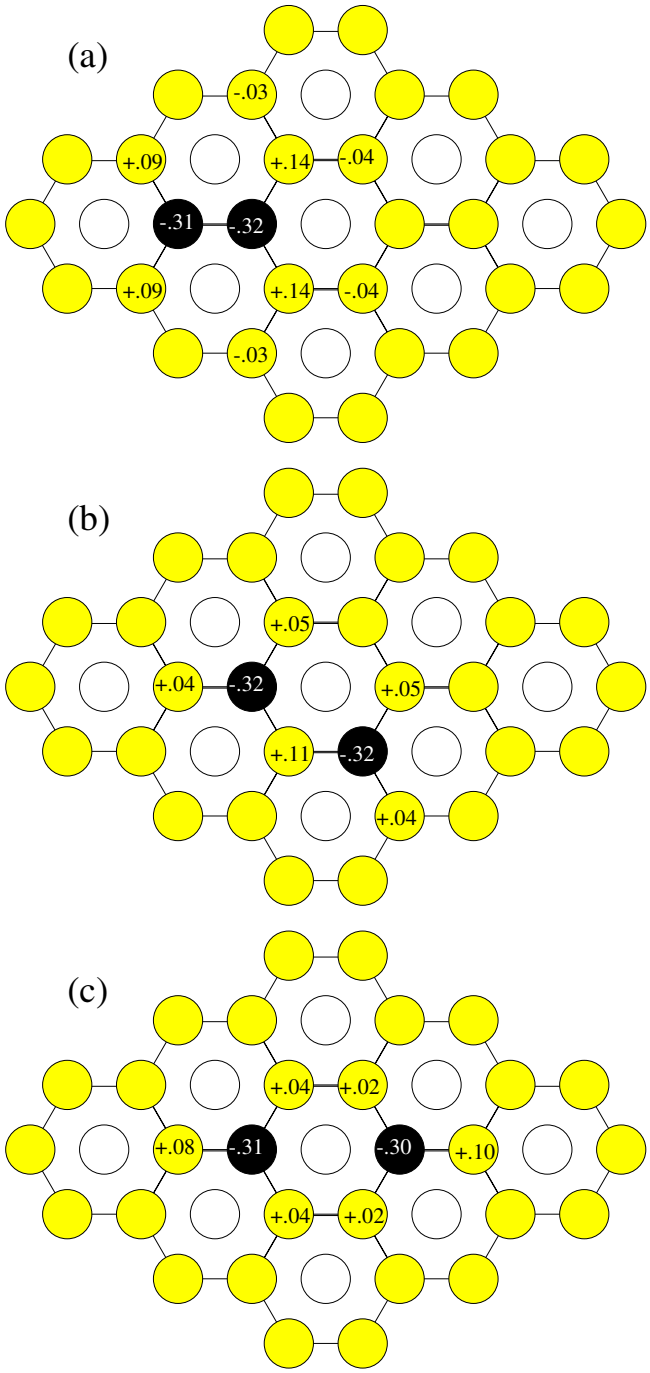

Figure 2. Relaxed structures (as in figure 1) for two Ge defects on first-nn (a), second-nn (b) and third-nn (c) positions.

provides, at LT, an STM image with a threefold symmetry, while at high T, the dynamical fluctuations between the two degenerate states (with different Sn atoms in the upper positions)

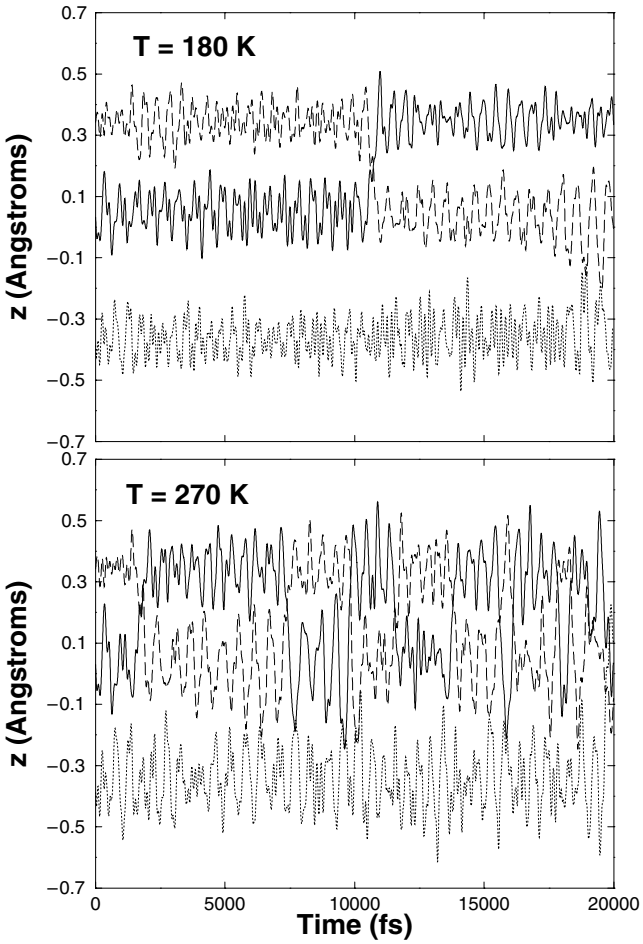

Figure 3. Time evolution of the z-coordinate of the surface atoms (two Sn atoms and the Ge substitutional: dotted curve) on the 3×3 unit cell in MD simulations at 180 and 270 K.

would yield the sixfold symmetry observed in the experiments. These dynamical effects, together with the upward displacement and the increased DB occupancy, are responsible of the enhanced brightness of the Sn atoms around the defect. Finally, the ordering of Ge defects at LT is naturally explained as an effect of the 3×3 reconstruction.

Acknowledgments

This work was partly funded by the Spanish CICYT under contract No PB-97-0028. Some of the calculations were performed in the CCC-UAM.

References

[1] Carpinelli J M *et al* 1996 *Nature* **381** 398
[2] Carpinelli J M *et al* 1997 *Phys. Rev. Lett.* **79** 2859
[3] Pérez R, Ortega J and Flores F 2001 *Phys. Rev. Lett.* **86** 4891

[4] Avila J *et al* 1999 *Phys. Rev. Lett.* **82** 442
[5] Ortega J, Pérez R and Flores F 2000 *J. Phys.: Condens. Matter* **12** L21
[6] de Gironcoli S *et al* 2000 *Surf. Sci.* **454–456** 172
[7] Jurczyszyn L, Ortega J, Pérez R and Flores F 2001 *Surf. Sci.* **482–5** 1350
[8] Melechko A *et al* 1999 *Phys. Rev. Lett.* **83** 999
[9] Weitering H H *et al* 1999 *Science* **285** 2107
[10] Melechko A *et al* 2000 *Phys. Rev.* B **61** 2235
[11] Clarke L J, Stich I and Payne M C 1992 *Comput. Phys. Commun.* **72** 14
[12] Demkov A A, Ortega J, Sankey O F and Grumbach M P 1995 *Phys. Rev.* B **52** 1618
Sankey O F and Niklewski D J 1989 *Phys. Rev.* B **40** 3979